ENVIRONMENTAL RESEARCH
LETTERS

LETTER · OPEN ACCESS

Using high resolution climate models to explore future changes in post-tropical cyclone precipitation

To cite this article: Erica Bower and Kevin A Reed 2024 *Environ. Res. Lett.* **19** 024042

ENVIRONMENTAL RESEARCH
LETTERS

OPEN ACCESS

RECEIVED
31 August 2023

REVISED
11 December 2023

ACCEPTED FOR PUBLICATION
22 January 2024

PUBLISHED
6 February 2024

LETTER

Using high resolution climate models to explore future changes in post-tropical cyclone precipitation

Erica Bower* **and Kevin A Reed**

Stony Brook University School of Marine and Atmospheric Sciences, 100 Nicholls Road, Stony Brook, NY 11794, United States of America

* Author to whom any correspond ence should be addressed.

E-mail: erica.bower@noaa.gov

Keywords: tropical cyclones, climate modeling, extratropical transition, extreme precipitation

Supplementary material for this article is available online

Abstract

One of the most costly effects of climate change will be its impact on extreme weather events, including tropical cyclones (TCs). Understanding these changes is of growing importance, and high resolution global climate models are providing potential for such studies, specifically for TCs. Beyond the difficulties associated with TC behavior in a warming climate, the extratropical transition (ET) of TCs into post-tropical cyclones (PTCs) creates another challenge when understanding these events and any potential future changes. PTCs can produce excessive rainfall despite losing their original tropical characteristics. The present study examines the representation of PTCs and their precipitation in three high resolution (25–50 km) climate models: CNRM, MRI, and HadGEM. All three of these models agree on a simulated decrease in TC and PTC events in the future warming scenario, yet they lack consistency in simulated regional patterns of these changes, which is further evident in regional changes in PTC-related precipitation. The models also struggle with their represented intensity evolution of storms during and after the ET process. Despite these limitations in simulating intensity and regional characteristics, the models all simulate a shift toward more frequent rain rates above 10 mm h^{-1} in PTCs. These high rain rates become 4%–12% more likely in the warmer climate scenario, resulting in a 5%–12% increase in accumulated rainfall from these rates.

1. Introduction

Tropical cyclones (TCs) are prolific rain producers both in the deep tropics and the subtropics. Additionally, the warming climate could cause individual storms to produce more rainfall than during past climate conditions [18, 30, 31]. As TCs move into the midlatitudes, they and their precipitation fields are affected by the process of extratropical transition (ET) through which TCs lose their tropical characteristics and become extratropical cyclones [5, 9], referred to as post-tropical cyclones (PTCs). The ET process is often defined using a cyclone phase space (CPS), as introduced in Hart [9], which determines the thermal symmetry and warm or cold core nature of the storm using geopotential height gradients. As a storm begins ET, the storm can develop fronts and become thermally asymmetric while losing its warm core characteristics [9]. This evolution of the storm causes the precipitation field of the TC to become asymmetric as it shifts to the left of the track of the storm in the Northern Hemisphere [13, 19]. Once a TC completes ET, the effects of the storm, such as high winds and heavy rainfall, can be felt far downstream of the traditional TC basins [2, 3, 7, 9, 35–37]. Despite the far reaching effects of such storms, PTCs and their precipitation have not been as widely studied as TCs. However, new analysis approaches have made the isolation of PTC precipitation easier [3]. This approach can be applied to large datasets, such as climate model output.

Advances in computational power enable high resolution climate modeling with grid spacing of 50 km or finer. These climate models can better simulate

storm-scale phenomena, particularly TCs [20, 33, 44]. The Coupled Model Intercomparison Project Phase 6 (CMIP6; Eyring *et al* [6]) devoted a subset of experiments, the High Resolution Model Intercomparison Project (HighResMIP) [8], to investigating the effect of horizontal resolution on the representation of TCs in climate models. Several studies have examined HighResMIP simulations to evaluate the accuracy with which the models can simulate TCs. Roberts *et al* [33] finds that increased horizontal resolution improves global TC frequency and intensity simulation HighResMIP models. Furthermore, higher resolution models are able to simulate TCs with smaller, more intense inner cores, a structure more similar to observed TCs than produced by the low resolution counterparts [33]. Li *et al* [20] finds that HighResMIP model simulations are able to simulate more realistic TC lifetimes, intensity, and genesis frequency than their low resolution counterparts. The effects of horizontal model resolution are also evident in the simulation of TC precipitation. Zhang *et al* [48] finds that many HighResMIP models produce higher TC rainfall totals with increased resolution. Most of the high resolution models in Zhang *et al* [48] performed better than their low resolution counterparts in simulating the global fraction of precipitation resulting from TCs, although biases remain at the basin scale.

Given these advances, HighResMIP models have been utilized to explore potential changes in future TC activity. Roberts *et al* [34] found a reduction in Southern Hemisphere TC activity and a poleward shift in the latitude of storm lifetime maximum intensity. Huang *et al* [11] also found more landfalling TCs in the West North Pacific and the North Atlantic. TC precipitation is found to change as well, with Huang *et al* [11] finding increased TC precipitation in all basins in the warming climate scenario. Similarly, Zhao [49] found increases in TC precipitation and the fraction of both extreme and all precipitation resulting from TCs reaching as far poleward as 50° N. This result highlights the impacts of TCs even at the end of their life cycles. Yet, PTCs have not been extensively examined in these high resolution models.

Outside of HighResMIP activities, studies have begun to examine projections of the ET process in a warmer world. Jung and Lackmann [15] used quasi-idealized atmosphere model simulations to show that warmer SSTs result in stronger TCs before ET occurs, longer durations of ET, and weaker storms after ET. Jung and Lackmann [14] also finds that simulations of Hurricane Irene in a warmer climate produce a longer ET process and increased precipitation depending on factors such as terrain. In 10-year atmospheric model simulations with future RCP8.5 forcing (a high-emissions future scenario from CMIP5; [38]), Michaelis and Lackmann [23] find that the percentage of storms that complete ET in the Northern Hemisphere increases by 5%–8% paired with a poleward shift in TC and ET activity. Building on this study, Michaelis and Lackmann [24] find an increase in precipitation intensity and areal coverage during and after ET completion. However, the same study finds less drastic changes for similar storms in the West North Pacific, highlighting the need to study basin-specific changes with warming. Finally, Baker *et al* [1] specifically examined ET in the HighResMIP models, focusing on potential changes of ET frequency and storm intensity in a warming climate. This study finds opposing shifts in ET latitude between the coupled and atmosphere-only models. All models used in Baker *et al* [1] agree on an increase in the number of ET occurrences in the North Atlantic and a decrease in the West North Pacific. Additionally, all models tended to produce stronger warm cores and more intense pre-ET storms with higher wind speeds, consistent with Michaelis and Lackmann [23].

Despite these recent studies focusing on the changes in ET in the future, few have examined PTC precipitation. The goal of the present study is to examine the representation of global PTC precipitation and activity in HighResMIP models and examine potential future changes in PTC precipitation. The remainder of this manuscript is structured as follows: section 2 describes the data and methods used. Section 3 details the results found in our analysis. Finally, section 4 provides some discussion and conclusions drawn from the previous section.

2. Data and methods

2.1. Climate models

The HighResMIP models used for this study include CNRM-CM6-1-HR (referred to throughout as CNRM; [43]), MRI-AGCM3-2-H (MRI; [25]), and HadGEM3-GC31-HM (HadGEM; [32]). These models were chosen based on the analysis of Roberts *et al* [33] and Roberts *et al* [34], which compared the representation of TCs in various HighResMIP models to the observed climatology. As in Roberts *et al* [33], CNRM is assessed due to its ability to simulate an accurate global TC frequency including Category 2 and 3 TCs (table 2). MRI is used in this study due to its ability to produce a wider range of TC intensities, including storms with wind speeds up to 80 m s^{-1} [34]. HadGEM is used for its fairly accurate distribution of TCs around the world, despite its overproduction of storms in the Southern Hemisphere. From Roberts *et al* [33] and Roberts *et al* [34], EC-Earth3P and MPI-ESM1 are excluded for their underproduction of TCs globally, CMCC-CM2 is not included due to the lack of availability of variables necessary for the tracking used in this study, and ECMWF-IFS is

Table 1. Overview of the observational and model datasets used. The dataset identifier is given in column 1, with dataset type in column 2. Column 3 specifies the spatial resolution of each dataset. Column 4 indicates temporal resolution. Column 5 lists the years of data that are used from each dataset.

Dataset	Type	Spatial	Temporal	Years used
IMERG	Observations	0.1°	30 min	2001–2019
ERA5	Reanalysis	0.25°	Hourly	2001–2019
IBTrACS	Observations	No Grid	6 hourly	2001–2019
CNRM	HighResMIP	0.5°	6 hourly/Daily	1950–2014, 2015–2048
MRI	HighResMIP	0.56°	6 hourly	1950–2014, 2015–2048
HadGEM	HighResMIP	0.23°	3 hourly	1950–2014, 2015–2048

not included due to the lack of availability of warming climate simulations [33]. For all three selected models, the 'highresSST' atmosphere only runs are utilized for both the historical (1950–2014) and the future (2015–2048) simulations [8]. The future simulations are forced with RCP8.5 warming forcing as in the CMIP5 experiments, causing the global average surface temperature to warm by 1.1 °C–1.2 °C in the future simulations compared to the historical simulations. CNRM and MRI have a 6 hourly temporal resolution with comparable spatial resolutions of 0.5° and 0.56° respectively. HadGEM has 3 hourly resolution which is downsampled to match the other models, with 0.23° latitude and 0.31° longitude spatial resolution (table 1).

While the high resolution model runs of each of the three selected models improved some aspects of the mean biases observed in their low resolution counterparts, especially in regard to TC simulation, some biases still remain in each model's mean simulated precipitation. For example, CNRM and HadGEM, even when upgraded to high resolution, tend to overproduce precipitation globally, with positive bias scores on the order of 0.3–0.5 [26]. MRI tends to produce too little rainfall along the Gulf coast of the United States in the summer months of June, July and August [45], and underestimates rainfall in parts of western Africa [27]. On the other hand, MRI overproduces rainfall in central Asia [21]. There is a range in the performance of the various HighResMIP models in their ability to simulate the mean global state as well as in simulation of TCs globally.

2.2. Observations

Comparisons of the historical model simulations to observations are completed using results from Bower *et al* [3], which constructed an observational climatology of PTC-related precipitation using observed TC trajectories from the International Best Track Archive for Climate Stewardship (IBTrACS; [16, 17]) that were extended to include post-ET points [46] and co-located with the Integrated Multi-Satellite Retrievals for GPM (IMERG) observational precipitation product [12]. Tracking of post-tropical points in the observational TC life cycles was completed using the ERA5 renalaysis dataset [10]. Additional details for these datasets can be found in table 1.

2.3. Methods

The methodology utilized for this study follows the framework introduced in Bower *et al* [3] with the addition of TC tracking. TCs are tracked using TempestExtremes [41, 42], which identifies sea level pressure minima with closed contours of pressure that satisfy a warm core criterion based on the geopotential height difference between 500 and 300 hPa. Settings, which are identical to the optimized settings in Ullrich and Zarzycki [42], can be found in appendix A of Bower *et al* [3]. Once TCs are tracked, ExTraTrack [46] is used to extend all TC trajectories to include points during and after ET until the extratropical cyclone fully dissipates. The ET process is defined within ExTraTrack using the CPS as in Hart [9]. ExTraTrack stops tracking a PTC when its central pressure rises above 1020 hPa, when 14 days have passed since ET completion, when translational speed exceeds 40 m s^{-1}, or when changes in direction exceed various thresholds, depending on translational speed ([46], adapted from Hart [9]). All points where topography exceeds 1000 m are masked out to prevent the tracking of topographic lows.

Precipitation objects are then tracked by TempestExtremes using thresholds of 1 mm h^{-1} and the 95th percentile of all 6 hourly rain rates at each location. Next, the radius over which to extract TC and PTC precipitation is generated by finding the locations around the storm center where the 500 hPa geopotential height rises by 10 m from the value at the storm center. A 1° great circle distance minimum mask is also imposed to ensure that strong TCs are included, but the variable mask is able to take on any shape, enabling the analysis of both symmetric and asymmetric storms. Finally, all precipitation objects that overlap the mask at any point are isolated as TC- or PTC-related precipitation objects. From the isolated precipitation field, composites are generated and shown in the supplemental material. Because HadGEM data has different spatial resolution in the latitude and longitude directions, the data was remapped to the MRI grid using TempestRemap

[39, 40] to create the composites. Further details on the methodology can be found in Bower *et al* [3].

Times before ET onset as defined by the CPS calculation [9] in ExTraTrack [46] correspond to a symmetric warm core and are considered 'pre-ET' in our analysis. When a storm is either an asymmetric warm core or a symmetric cold core in the CPS, it is considered 'during-ET.' Once a storm is determined by the phase space to be an asymmetric cold core, the storm is then labeled as 'post-ET'. For the remainder of this manuscript, the term 'PTC' refers to all times after the onset of ET.

3. Results

Using this methodology to isolate the asymmetric precipitation associated with PTCs, we are able to complete a novel investigation of PTC precipitation in high resolution climate models. We begin by assessing ET representation and comparing to prior work before addressing the rainfall resulting from PTCs.

3.1. PTC Frequency

Observations indicate that 33.2% of all global TCs completed ET between 2001 and 2019. All three models underestimate the percentage of TCs that undergo ET to varying degrees (table 2). However, this single metric is not fully indicative of the accuracy of each model's representation of ET events. For example, CNRM's percentage is heavily skewed by the model's overproduction of TC (figure S1) and ET activity in the North Indian basin (NIND), as noted in Roberts *et al* [33, 34] for TC activity. Only 8% of the observed Northern Hemisphere (NH) TC activity occurs in the NIND, but CNRM historical runs simulate 18.8% of NH storms in the basin (figure S1). These biases persist into ET occurrence as well (figure 1). MRI also overproduces TC and PTC activity in the NIND, but not to the extent that CNRM does. HadGEM, on the other hand, overproduces TCs (figure S1) and ET events (figure 1) in the Pacific Ocean and in the Southern Hemisphere (SH). These results are consistent with prior work [1, 33, 34, 48]. Regardless of these spatial and frequency biases, CNRM and MRI capture a distinct seasonal cycle of both TC and PTC activity with the seasonal peak of PTC activity slightly early (figure S2). HadGEM's TC seasonal cycle is more uniform throughout the year, largely due to its overproduction of TC activity in the SH (figure S1). However, this allows HadGEM to simulate the bimodal seasonal cycle of PTCs better than the other two models (figure S2).

Aside from the overproduction of TC and PTC activity in the NIND, CNRM underrepresents ET events elsewhere (figure 1), producing less than half of the observed events per year in the North Atlantic (NATL) and the West North Pacific (WPAC). MRI also underestimates PTC events, with only 1-2 events per year in the NATL and in the SH, particularly near Madagascar. Conversely, HadGEM overproduces PTCs in the Pacific basins and represents NATL activity most accurately of the three models (figure 1). In the SH, CNRM and MRI produce an accurate number of events along the Australian coastlines, while HadGEM again overproduces (figure 1).

Looking to a warmer mean state climate, the changes simulated are rather noisy. Even areas with statistically significant changes between the future and historical simulated mean track density (stippling in figure 1 rightmost column) are inconsistent among the models. All models agree on an increase in events, with differing magnitudes, west of Australia. Similar to the results of Baker *et al* [1], we find an increase or no change in ET occurrence in the NATL consistent among the models, particularly near western Europe (figure 1). When examining the global changes, all three models agree on a simulated decrease in the global number of TC and ET events in the future simulations (table 2; figure 1). This consistency provides some confidence in simulated changes in the frequency of events, despite the mixed results concerning the duration of the ET process and the percentage of TCs that undergo ET. CNRM and HadGEM are able to simulate a more realistic duration of ET, but both models show little change in ET duration in future simulations. MRI produces shorter ETs in the warmer scenario (table 2), similar to the results of Jung and Lackmann [15]. The percentage of storms that undergo ET each year does not change much in the CNRM and MRI future scenario. On the contrary, HadGEM shows a 4.8% increase in the percentage of storms that undergo ET. While the models' simulated percentage changes remain inconclusive, these changes may suggest that the decrease in ET events in the future is driven by the reduction in the overall number of TCs per year in the warmer simulations (table 2).

3.2. PTC intensity

We next examine the simulation of the intensity of storms before, during, and after the ET process. Cases such as Hurricane Sandy (2012) illustrate how the use of sea level pressure rather than 10 m wind speeds is a more accurate determination of storm strength in the broad wind fields characteristic of ET storms [4]. Thus, we use central pressure as our definition of TC or PTC intensity.

In observations (black lines, figure 2), the intensity distribution of storms before ET onset and after ET completion is left skewed with a peak near 1000 hPa. During ET, the distribution takes on a flatter shape with a maxima near 990 hPa and 950 hPa. A

Table 2. Climatology by dataset. Average number of TCs and ET events per year are given in columns 2 and 3. The total percentage of storms that undergo ET during the time frame of each dataset is given in column 4. The average duration of the ET process in hours is given in column 5.

Dataset	TCs/yr	ETs/yr	% of TCs that ET	ET Duration (h)
IBTrACS	97.7	32.5	33.2%	82.3
CNRM-Hist	102.9	30.7	$31.4\% \pm 0.7\%$	61.3
CNRM-Futr	88.6	26.3	$29.5\% \pm 1.1\%$	61.6
MRI-Hist	70.9	20.0	$28.4\% \pm 0.7\%$	47.6
MRI-Futr	65.4	18.4	$28.2\% \pm 1.0\%$	43.4
HadGEM-Hist	246.4	48.7	$19.8\% \pm 0.3\%$	63.1
HadGEM-Futr	175.5	42.9	$24.4\% \pm 0.6\%$	66.2

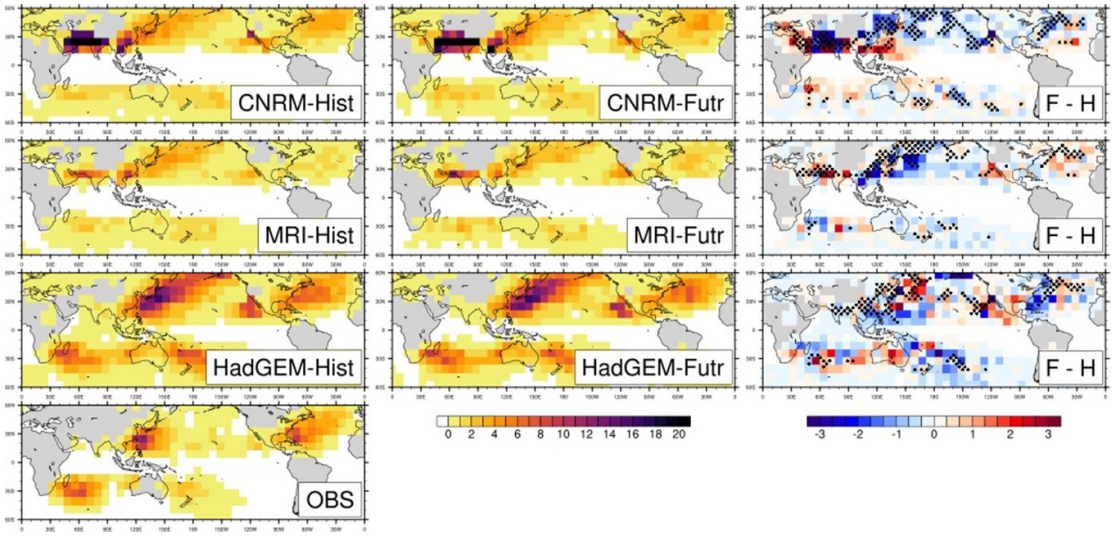

Figure 1. Number of 6 hourly occurrences of PTCs per year. Row 1: CNRM historical (CNRM-Hist), CNRM future (CNRM-Futr), and difference (F)–(H) between future and historical. Row 2: as in row 1, for MRI. Row 3: As in rows 1-2, for HadGEM. Row 4: observations. All datasets are mapped to an 8° lat/lon grid, as in Zarzycki *et al* [47]. Spatial correlations between the historical simulations and observations are 0.09, 0.38, and 0.65 for CNRM, MRI, and HadGEM respectively, shown in figure S3. Stippling in the difference panels indicates where the differences are statistically significant to the 66% level using a two sample t-test for the difference of means. The 66% level was chosen based on the Intergovernmental Panel on Climate Change's definition of a 'likely' scenario [22].

more even intensity distribution is also observed in Hart [9] during the ET process. All three models fail to capture this distribution during the ET process, instead retaining the left skewed shape similar to the pre- and post-ET phases. CNRM tends to have slightly stronger storms before ET onset compared to observations, while MRI and HadGEM have median values similar to observations or slightly weaker. All models also show a shift toward weaker storms in the pre-ET phase in the warmer future simulations for storms that undergo ET. Once ET begins, these models struggle to capture the observed intensity evolution of the storm. Both MRI and CNRM project slightly lower pressure medians in the warmer scenario post-ET, while HadGEM shows weaker post-ET storms. However, all of the future simulations' median intensities fall within the range of the statistical uncertainty of the same model's historical simulations' median intensities, leaving little confidence in the likelihood of these changes appearing consistently. Overall, the models are able to simulate a realistic distribution of TC intensities before ET begins but struggle throughout the ET process. The simulated intensities of these storms may impact the evolution of the rain field throughout the ET process.

3.3. PTC precipitation

The biases in PTC track density impact the simulation of average annual PTC precipitation (see figure 3 for 95th percentile results, results for 1 mm h^{-1} shown in figure S4). There is an overall under-representation of PTC precipitation in CNRM and MRI due to the lack of production of ET events (i.e. figure 1). Although HadGEM overproduces TC and PTC activity, it still slightly underestimates 95th percentile PTC precipitation in most areas.

Each model also varies in its simulated changes in the future warming scenario (figure 3). While MRI

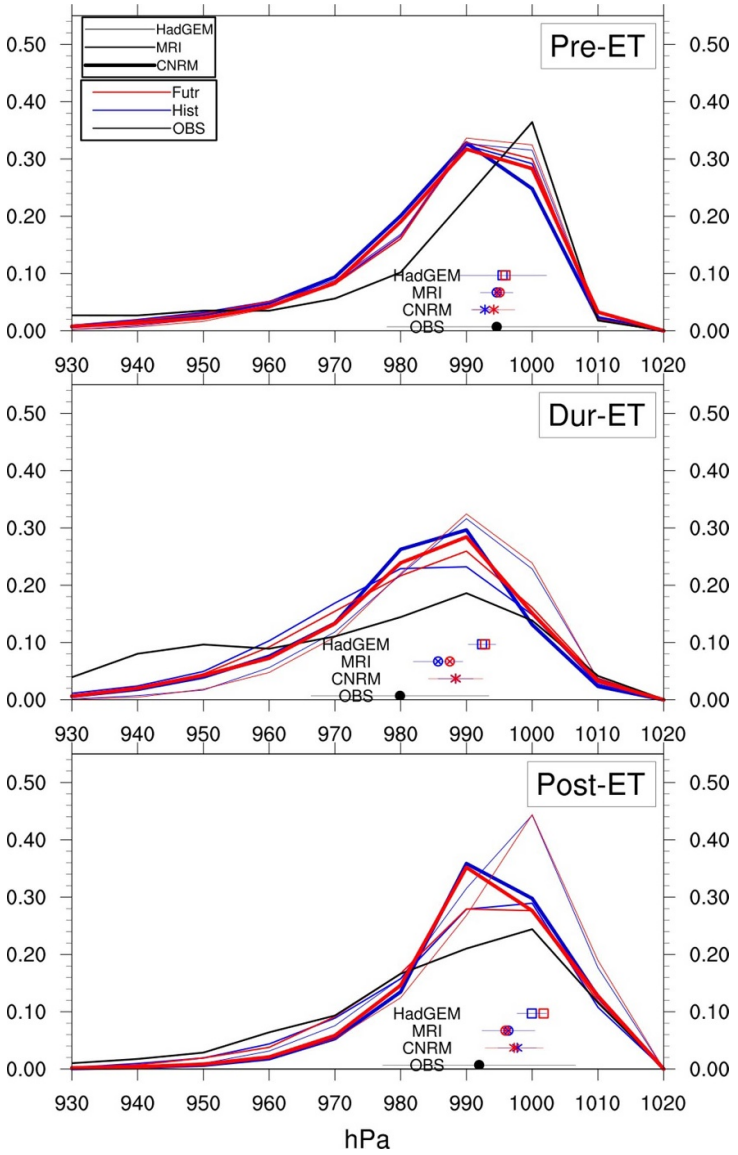

Figure 2. Relative frequency of 6 hourly occurrences of a storm reaching each intensity (hPa). Top panel before ET onset. Middle panel: during ET. Bottom panel after ET completion. Blue lines indicate historical simulations, red lines indicate future simulations, and black lines indicate observations. Various line thicknesses distinguish between the models used. Markers beneath the curves show the median of the distribution for each curve, with different shapes corresponding to the different models and observations. Lines extending from the median markers indicate the statistical uncertainty in the median value for each set of model simulations.

in general produces a worldwide increase in PTC precipitation in the future scenario, the other two models have more basin-dependent patterns. CNRM and MRI simulate higher average PTC rainfall in the future simulations in the NATL, while HadGEM shows a small area of increased PTC precipitation surrounded by decreased rainfall in the same basin. All three models indicate slight increases and decreases in PTC rainfall juxtaposed in the WPAC. Since a similar pattern is seen in PTC track density, this may represent a shift in the PTC activity away from the east coast of Asia. Unlike the other two models, HadGEM suggests a slight increase in PTC precipitation in the highest NH latitudes, simulating more storms that reach high latitudes. Also noteworthy is that CNRM and MRI agree upon an increase in PTC precipitation in western Europe in the warming climate scenario despite little to no change in the number of events (figure 1). This indicates that the precipitation per storm could increase in the downstream areas.

Examining all storms regardless of spatial distribution reveals some consistency among the models in simulated changes in the warmer climate scenario. All three models agree on increased rain rates above 1 mm h^{-1} in the pre-ET phase of storms in a warmer mean state (figures S5–S8), but uncertainty remains in the during- and post-ET phases when using this

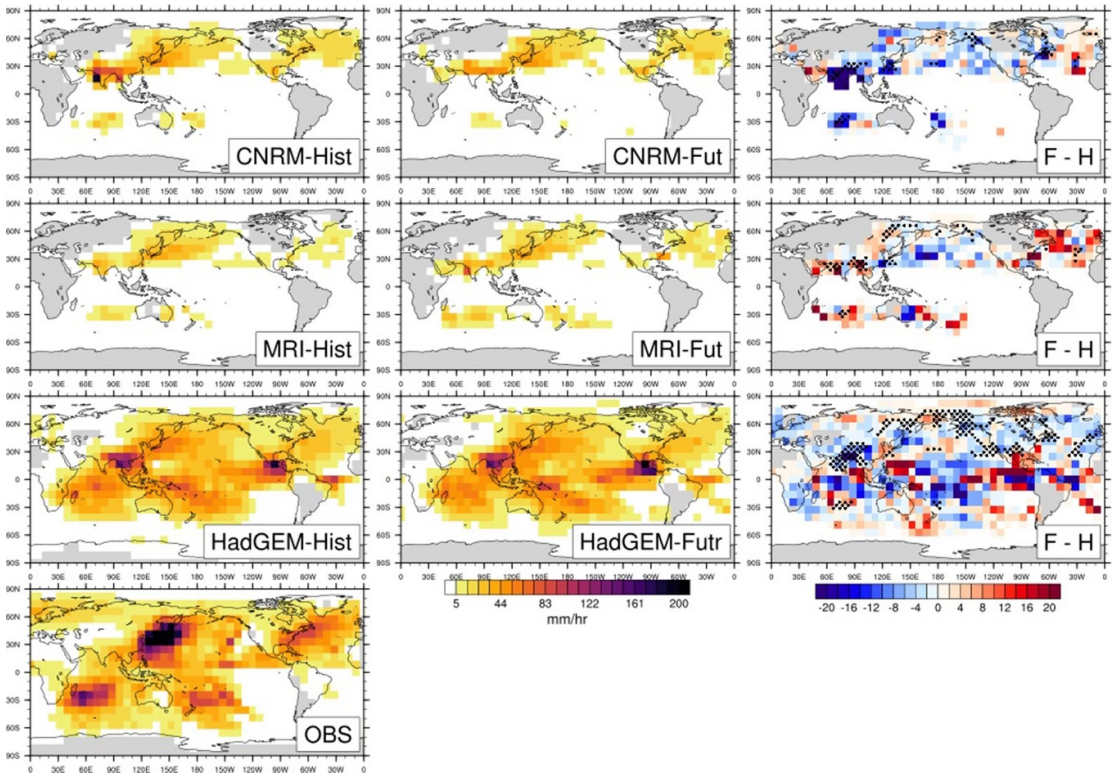

Figure 3. Average annual accumulated PTC-related precipitation using the 95th percentile threshold for precipitation tracking. Historical simulations are shown in the left column with observations shown on the bottom left, future simulations in the center column, and the difference between the future and historical averages in the rightmost column. Stippling in the difference panels indicates where the differences are statistically significant to the 66% level using a two sample t-test for the difference of means.

approach. The full distribution of PTC rainfall from the during- and post-ET phases reveals some consistency among the models when comparing the warmer climate simulations to the historical. Figure 4 shows the frequency proportion and accumulated precipitation of each rain rate (mm h^{-1}) for each set of model simulations using a 1 mm h^{-1} threshold following the methodology of Pendergrass and Hartmann [28]. Blue lines in figure 4 indicate the historical simulations, while red lines indicate the future simulations. In each model, the peak rain rate simulated within PTCs during and after the ET process is between 1 and 4 mm h^{-1} with the frequency of occurrence of rain rates greater than 4 mm h^{-1} decreasing rapidly with increasing rain rate. The bulk of the accumulated rainfall can be attributed to the rain rates between 3 and 4 mm h^{-1} in MRI and HadGEM, with CNRM's peak of accumulated rainfall resulting from 5 mm h^{-1} rain rates. At the low rain rates, all three models simulate a decrease in the frequency of rain rates less than 5 mm h^{-1} in the warmer mean state simulations. However, when focusing on the right tail of the distribution in the right two panels of figure 4, it becomes evident that all models show an increase in the frequency of rain rates occurring above 10 mm h^{-1}. These high rain rates are simulated to become 4%–12% more likely in the warmer climate scenario, leading to increased accumulated rainfall by 5%–12% from rain rates of 10 mm h^{-1} and greater, depending on the model. Therefore, the thermodynamic effect of 1.1 °C–1.2 °C of warming on PTC rainfall is evident in the shift from lighter to heavier rain rates and increased accumulated rainfall from heavier rain rates within these storms.

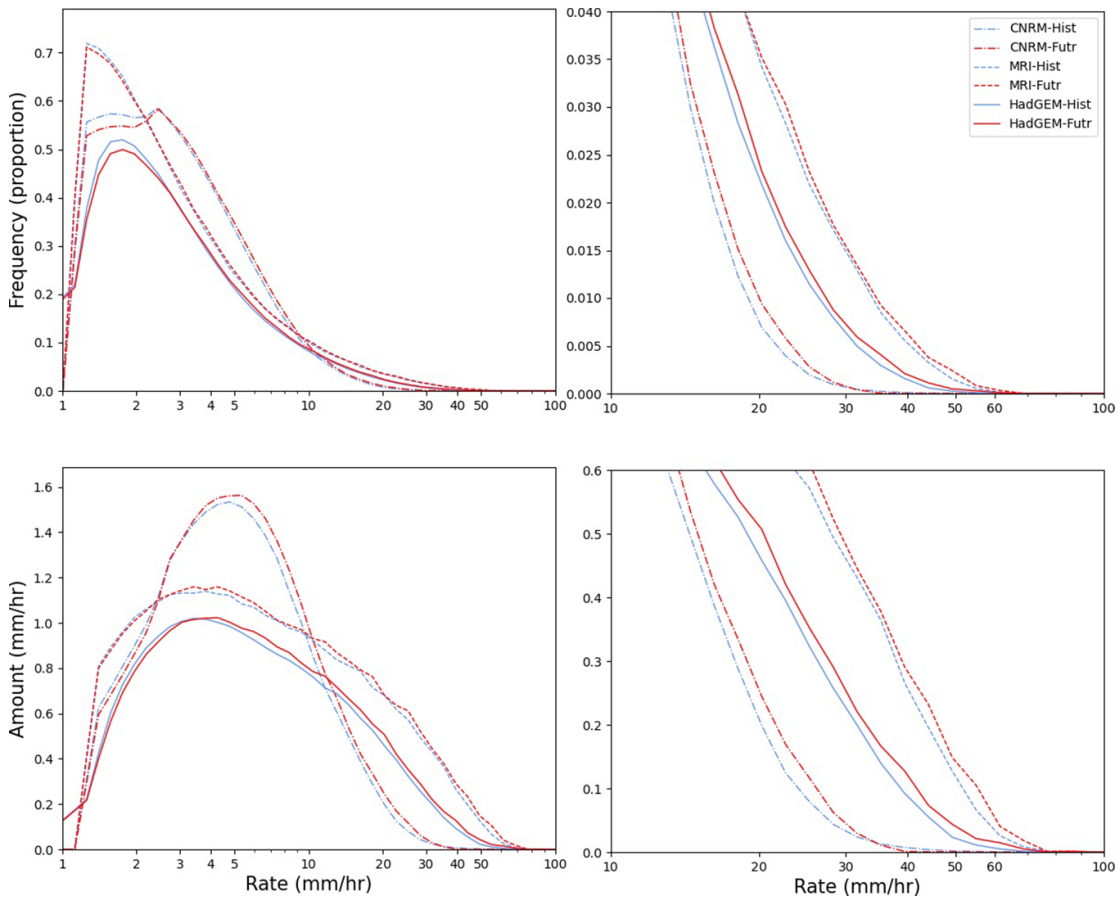

Figure 4. Distributions of PTC precipitation (during and post-ET phases) for each of the HighResMIP model simulations. The top panels show the frequency proportion at each rain rate (mm/hr) with the bottom panels showing the accumulated rainfall resulting from rainfall at each rain rate. The right side simply shows a closer view of the right tail of the distributions from the left side. Blue lines indicate historical while red lines indicate future simulations. The different models are distinguished by different dash patterns.

4. Summary and discussion

This study constructed the first global analysis of PTC occurrence and rainfall in three HighResMIP models, including CNRM, MRI, and HadGEM. Overall, the frequency of the ET process is underrepresented by these models, while the percent of TCs in the simulations that undergo ET is only underestimated by 2%–5% in CNRM and MRI with HadGEM's percentages straying farther from observed values. The relative spatial distributions of TC and PTC tracks mirror each other, suggesting that biases in ET simulation arise from biases in TC activity. All three models also struggle to represent the intensity distribution of storms in the during- and post-ET phases, keeping storms too weak once the ET process begins.

Despite these biases, all three models agree that the global number of TC and ET events would decrease in a warmer mean state climate scenario, but the regional changes in frequency remain uncertain. Biases in activity translate to the rainfall associated with the storms as well. Aside from the commonly affected areas like the east coasts of continents, downstream areas may also see changes in these quantities in a warmer world. Both CNRM and MRI indicate that although the number of events does not change in the future simulations, the precipitation resulting from PTCs increases near Western Europe. These, among other issues that could potentially arise from the warming climate, must be considered when managing infrastructure growth in coastal areas around the world.

There is some consistency among the models in determining changes in precipitation when viewed from a storm-centric perspective rather than the global distribution of PTC rainfall. All three models agree on a shift from lighter precipitation rates under 5 mm h^{-1} within PTCs both during and after the ET process to heavier rain rates above 5 mm h^{-1} and increased accumulated rainfall resulting from these heavier rain rates in a warmer mean state climate. This shift from lighter to heavier rainfall could contribute to increases in per-event precipitation, as simulated by the models in some parts of the world. Areas impacted by these storms may face heavier rain rates within certain regions of the PTC, which may exacerbate some impacts of PTC rainfall. As population and infrastructure continue to increase in coastal

areas [29], this could leave a greater number of people more vulnerable to flooding caused by PTC rainfall as storms reach the mid- and high latitudes.

The lack of clear regional agreement amongst the models indicates a need for more targeted high resolution climate modeling efforts. These projects have greatly improved TC representation in climate simulations, with prior work such as Roberts *et al* [33], Li *et al* [20], and Baker *et al* [1] showing the improvements made by increasing horizontal model resolution. This work must be continued and extended to also determine how the simulation of TC interactions with the midlatitude environment can also be improved in the coming years. The correction of some biases in TC activity will likely lead to improvements in the representation of PTC activity in the models as well. While the primary goal of HighResMIP was to determine the effects of resolution on the representation of phenomena like TCs in global climate models, the project intends to expand to study the effects of warming in future phases of HighResMIP. This shift of focus will allow for the targeted future study of the effect of the warming mean state on ET and the associated rainfall.

Data availability statement

All data that support the findings of this study are included within the article (and any supplementary files). The data that support the findings of this study are available at the following URLs:

IMERG Final Run: https://gpm1.gesdisc.eosdis.nasa.gov/data/GPM_L3/GPM_3IMERGHH.06/.

IBTrACS v4: www.ncdc.noaa.gov/ibtracs/index.php?name=ib-v4-access.

ERA5 reanalysis: https://cds.climate.copernicus.eu/#!/search?text=ERA5&type=dataset.

HighResMIP: https://esgf-index1.ceda.ac.uk/search/cmip6-ceda/

TempestExtremes: https://github.com/ClimateGlobalChange/tempestextremes.

ExTraTrack: https://github.com/zarzycki/ExTraTrack.

Acknowledgments

Bower and Reed acknowledge the funding support of NASA under Grant 80NSSC19K0717 and NSF under AGS2244917 and the high-performance computing resources of the National Energy Research Scientific Computing Center (NERSC). No conflicts of interest, real or perceived, financial or by affiliation, exist for any author. We thank the modeling groups within PRIMAVERA (a European Union Horizon 2020 project under Grant Agreement 641727) for producing the multi-model simulations and providing the climate model outputs via the Earth System Grid Federation (ESGF). We greatly appreciate Dr Malcolm Roberts and Dr Jon Seddon (U.K. Met Office Hadley Centre) for their help in accessing the model data through the UK Centre for Environmental Data Analysis's JASMIN platform (www.ceda.ac.uk/services/jasmin/).

We acknowledge the World Climate Research Programme, which, through its Working Group on Coupled Modelling, coordinated and promoted CMIP6. We thank the climate modeling groups for producing and making available their model output, the Earth System Grid Federation (ESGF) for archiving the data and providing access, and the multiple funding agencies who support CMIP6 and ESGF.

We would also like to thank the Calibrated and Systematic Characterization, Attribution, and Detection of Extremes (CASCADE) Scientific Focus Area at Lawrence Berkeley National Laboratory, funded by the Earth and Environmental System Modeling (EESM) Program in the DOE BER Earth and Environmental Systems Sciences Division (EESSD), for downloading and aggregating the HighResMIP data for our utilization.

References

[1] Baker A J *et al* 2022 Extratropical transition of tropical cyclones in a multiresolution ensemble of atmosphere-only and fully coupled global climate models *J. Clim.* **35** 5283–306

[2] Bieli M, Camargo S, Sobel A, Evans J and Hall T 2019 A global climatology of extratropical transition. Part I: Characteristics across basins *J. Clim.* **32** 3557–82

[3] Bower E, Reed K A, Ullrich P A, Zarzycki C M and Pendergrass A G 2022 Quantifying heavy precipitation throughout the entire tropical cyclone life cycle *J. Hydrometeorol.* **23** 1645–62

[4] Chavas D R, Reed K A and Knaff J A 2017 Physical understanding of the tropical cyclone wind-pressure relationship *Nat. Commun.* **8** 1360

[5] Evans C *et al* 2017 The extratropical transition of tropical cyclones. Part I: cyclone evolution and direct impacts *Mon. Weather Rev.* **145** 4317–44

[6] Eyring V, Bony S, Meehl G A, Senior C A, Stevens B, Stouffer R J and Taylor K E 2016 Overview of the Coupled Model Intercomparison Project Phase 6 (CMIP6) experimental design and organization *Geosci. Model Dev.* **9** 1937–58

[7] Haarsma R 2021 European Windstorm risk of post tropical cyclones and the impact of climate change *Geophys. Res. Lett.* **48** e2020GL091483

[8] Haarsma R J *et al* 2016 High resolution model intercomparison project (HighResMIP v1.0) for CMIP6 *Geosci. Model Dev.* **9** 4185–208

[9] Hart R 2003 A cyclone phase space derived from thermal wind and thermal asymmetry *Mon. Weather Rev.* **131** 585–616

[10] Hersbach H *et al* 2020 The ERA5 global reanalysis *Q. J. R. Meteorol. Soc.* **146** 1999–2049

[11] Huang H, Patricola C M and Collins W D 2021 The influence of ocean coupling on simulated and projected tropical cyclone precipitation in the HighResMIP-PRIMAVERA simulations *Geophys. Res. Lett.* **48** e2021GL094801

[12] Huffman G, Stocker E, Bolvin D, Nelkin E and Tan J 2019 WGPM IMERG Final Precipitation L3 Half Hourly 0.1 degree x 0.1 degree V06 (Goddard Earth Sciences Data and Information Services Center (GES DISC))

[13] Jones S *et al* 2003 The extratropical transition of tropical cyclones: forecast challenges, current understanding

and future directions *Weather Forecast.* **147** 1052–92
[14] Jung C and Lackmann G M 2019 Extratropical transition of Hurricane Irene (2011) in a changing climate *J. Clim.* **32** 4847–71
[15] Jung C and Lackmann G M 2021 The response of extratropical transition of tropical cyclones to climate change: quasi-idealized numerical experiments *J. Clim.* **34** 4361–81
[16] Knapp K R, Diamond H, Kossin J, Kruk M and Schreck C 2018 International Best Track Archive for Climate Stewardship (IBTrACS) project, version 4 (NOAA National Centers for Environmental Information)
[17] Knapp K R, Kruk M, Levinson D, Diamond H and Neumann C 2010 The International Best Track Archive for Climate Stewardship (IBTrACS): unifying tropical cyclone Best Track data *Bull. Am. Meteorol. Soc.* **91** 363–76
[18] Knutson T *et al* 2020 Tropical cyclones and climate change assessment: Part II: projected response to anthropogenic warming *Bull. Am. Meteorol. Soc.* **3** E303–22
[19] Konrad I I C Meaux M and Meaux D 2002 Relationships between tropical cyclone attributes and precipitation totals: considerations of scale *Int. J. Climatol.* **22** 237–47
[20] Li J *et al* 2021 Effect of horizontal resolution on the simulation of tropical cyclones in the Chinese Academy of Sciences FGOALS-f3 Climate System Model *Geosci. Model Dev.* **14** 6113–33
[21] Li L-L, Li J and Yu R C 2022 Evaluation of CMIP6 HighResMIP models in simulating precipitation over Central Asia *Adv. Clim. Change Res.* **3** 1–12
[22] Masson-Delmotte V *et al* 2021 *Climate Change 2021: The Physical Science Basis: Contribution of Working Group to the Sixth Assessment Report of the Intergovernmental Panel on Climate Change* vol 6 (Cambridge University Press) pp 3–32
[23] Michaelis A C and Lackmann G M 2019 Climatological changes in the extratropical transition of tropical cyclones in high resolution global simulations *J. Clim.* **32** 8733–53
[24] Michaelis A C and Lackmann G M 2021 Storm-scale dynamical changes of extratropical transition events in present-day and high-resolution global simulations *J. Clim.* **34** 5037–62
[25] Mizuta R, Yoshimura H, Ose T, Hosaka M and Yukimoto S 2019 MRI MRI-AGCM3-2-H model output prepared for CMIP6 HighResMIP (Earth System Grid Federation)
[26] Moreno-Chamarro E *et al* 2022 Impact of increased resolution on long-standing biases in HighResMIP-PRIMAVERA climate models *Geosci. Model Dev.* **15** 269–89
[27] Olabamiji Ajibola F and Abosede Afolayan S 2023 Impacts of improved horizontal resolutions in the simulations of mean and extreme precipitation using CMIP6 HighResMIP models over West Africa *Theor. Appl. Climatol.* (available at: https://www.researchsquare.com/article/rs-2917394/v1)
[28] Pendergrass A G and Hartmann D 2014 Changes in the distribution of rain frequency and intensity in response to global warming *J. Clim.* **27** 8372–83
[29] Pielke J R Landsea C, Mayfield M, Layer J and Pasch R 2005 Hurricanes and global warming *Bull. Am. Meteorol. Soc.* **86** 1571–6
[30] Reed K A, Stansfield A M, Wehner M F and Zarzycki C M 2020 Forecasted attribution of the human influence on Hurricane Florence *Sci. Adv.* **6** eaaw9253
[31] Reed K, Wehner M and Zarzycki C 2022 Attribution of 2020 hurricane season extreme rainfall to human-induced climate change *Nat. Commun.* **13** 1905
[32] Roberts M 2019 MOHC HadGEM3-GC31-HM model output prepared for CMIP6 HighResMIP (Earth System Grid Federation) (available at: https://doi.org/10.22033/ESGF/CMIP6.446)
[33] Roberts M J *et al* 2020 Impact of model resolution on tropical cyclone simulation using the HighResMIP-PRIMAVERA multimodel ensemble *J. Clim.* **33** 2557–83
[34] Roberts M J *et al* 2020 Projected future changes in tropical cyclones using the CMIP6 HighResMIP multimodel ensembles *Geophys. Res. Lett.* **47** e2020GL088662
[35] Sainsbury E M, Schniemann R K, Hodges K I, Baker A J, Shaffrey L C, Bhatia K T and Bourdin S 2022 Can low resolution CMIP6 ScenarioMIP models provide insight into future european post-tropical cyclone risk? *Weather Clim. Dyn.* **3** 1359–79
[36] Sainsbury E M, Schniemann R K, Hodges K I, Shaffrey L C, Baker A J and Bhatia K T 2020 How important are post-tropical cyclones for European windstorm risk? *Geophys. Res. Lett.* **47** e2020GL089853
[37] Stuivenvolt Allen J, Simon Wang S Y, LaPlante M D and Yoon J H 2021 Three Western Pacific typhoons strengthened fire weather in the recent northwest U.S. conflagration *Geophys. Res. Lett.* **48** e2020GL091430
[38] Taylor K E, Stouffer R J and Meehl G A 2012 An Overview of CMIP5 and the Experiment Design *Bull. Am. Meteorol. Soc.* **93** 485–98
[39] Ullrich P A, Devendran D and Johansen H 2016 Arbitrary-order conservative and consistent remapping and a theory of linear maps: part 2 *Mon. Weather Rev.* **144** 1529–49
[40] Ullrich P A and Taylor M A 2015 Arbitrary-order conservative and consistent remapping and a theory of linear maps: part 1 *Mon. Weather Rev.* **143** 2419–40
[41] Ullrich P A, Zarzycki C M, McLenny E E, Pinheiro M C, Stansfield A M and Reed K A 2021 TempestExtremes v2.1: a community framework for feature detection, tracking and analysis in large datasets *Geosci. Model Dev.* **14** 5023–48
[42] Ullrich P and Zarzycki C 2017 TempestExtremes: a framework for scale-insensitive pointwise feature tracking on unstructured grids *Geosci. Model Dev.* **10** 1069–90
[43] Voldoire A 2019 CNRM-CERFACS CNRM-CM6-1-HR model output prepared for CMIP6 HighResMIP (Earth System Grid Federation) (available at: https://doi.org/10.22033/ESGF/CMIP6.1387)
[44] Wehner M F *et al* 2014 The effect of horizontal resolution on simulation quality in the Community Atmosphere Model: CAM5.1 *J. Adv. Model. Earth Syst.* **6** 980–97
[45] Wehner M, Lee J, Risser M, Ullrich P, Gleckler P and Collins W D 2021 Evaluation of extreme sub-daily precipitation in high-resolution global climate model simulations *Phil. Trans. R. Soc.* **379** 20190545
[46] Zarzycki C M, Thatcher D and Jablonowski C 2017 Objective tropical cyclone extratropical transition detection in high-resolution reanalysis and climate model data *J. Adv. Model. Earth Syst.* **9** 130–48
[47] Zarzycki C M, Ullrich P A and Reed K A 2021 Metrics for evaluating tropical cyclones in climate data *J. Appl. Meteorol. Climatol.* **60** 643–60
[48] Zhang W *et al* 2021 Tropical cyclone precipitation in the HighResMIP atmosphere-only experiments of the PRIMAVERA project *Clim. Dyn.* **57** 253–73
[49] Zhao M 2021 A study of AR-, TS- and MCS-associated precipitation and extreme precipitation in present and warmer climates *J. Clim.* **35** 479–97